Hyperbolic Secant Coupling in Overmoded Waveguide

J. L. DOANE, MEMBER, IEEE

Abstract—This work presents a new solution of the coupled-mode equations for a hyperbolic secant spatial variation of the coupling between two modes. An analytic expression is given for the transmission coefficient for arbitrary complex differential propagation constant and coupling strength. The expression is particulary simple in the case when the differential attenuation between the modes is negligible.

Design curves are presented in terms of normalized parameters. The hyperbolic secant coupling may be truncated and still yield virtually the same transmission as for infinite couping length. The required coupling length is indicated by a comparison of the ideal expression with the results of numerical integration of the coupled-mode equations.

Hyperbolic secant coupling can be particularly useful for the design of short low-loss broad-band bends, twists, and mode-selective couplers in overmoded waveguide. Results of tests on 90-degree bends in rectangular and corrugated circular waveguide are consistent with the theory.

I. INTRODUCTION

ALTHOUGH the coupled-wave equations have a deceptively simple form, few analytical solutions have been found. A simple solution for arbitrary coupling variation exists when reflections may be neglected and when the two coupled modes are degenerate (that is, have the same propagation constants) [1]. When reflections are negligible and the coupling is constant, Miller [2] and Smith [3] have derived solutions for the case of constant and linearly tapered differences in propagation factors, respectively. For the case of arbitrary coupling variation and constant difference in propagation factors, Rowe [1] has used perturbation theory to derive solutions in the form of Fourier integrals, and Waldron [4] has developed solutions for slowly varying coupling based on Miller's constant coupling solution [2]. Miller's solution [2] has also been used as a basis for treating periodic coupling [5], [6] and random coupling [7].

In waveguide tapers, the coupling and propagation factors vary simultaneously. Solymar [8], [9] has developed estimates for the mode conversion in tapers with a linear profile, Unger [10] has developed a synthesis technique for broad-band tapers with low mode conversion using perturbation theory, and other approaches are described by Sporleder and Unger [11]. The case of a parabolic taper profile was treated in [12], and analytical solutions for this case were derived in [11] and [13].

Reflections have been considered in solutions for waveguides and transmission lines in which the coupled modes are not far from cutoff or the impedance is varying significantly. Solutions for these cases, and where forward mode conversion is impossible or unimportant, have been obtained by Hecken [14] (and earlier references cited therein) and Waldron [15] using formalisms similar to those in [10] and [4], respectively. A solution for both mode conversion and reflections in a coupler with degenerate modes and coupling with a Gaussian variation is described in [16].

This work presents a new analytic expression for the transmission coefficient for the amplitude of a mode initially having all the power and whose coupling with another mode has a hyperbolic secant variation. This expression is valid for arbitrary constant differential phase and attenuation factors when reflections are negligible. It reduces in the limit of small coupling to expressions derivable from perturbation theory for the same coupling variation, and in general predicts higher transmission (less mode conversion) than the perturbation theoretical expressions. In the case of negligible differential attenuation between modes, the exact expression for the power lost from the initial mode is separable into a product of the power that would be lost with zero differential phase constant and the square of a hyperbolic secant function of the differential phase constant.

Aside from its theoretical interest as a new analytic solution, the solution for hyperbolic secant coupling variation can be used to design short low-loss bends and twists in overmoded waveguide. Since the mode conversion is a monotonic function of the differential phase constant when the differential attenuation is negligible, the design of components with hyperbolic secant coupling is relatively simple. When a relatively broad-band component is required, the hyperbolic secant coupling variation also frequently provides lower mode conversion for a given length than other common coupling variations (constant coupling, linearly tapered or triangular coupling, cosine coupling, etc).

In the next section, we set up the coupled-wave equations describing the problem. The properties of the solution, derived in the Appendix, are discussed in Section III. Finally, Section IV presents some theoretical and experimental results for two examples of 90-degree bends in

Manuscript received January 11, 1984; revised April 8, 1984. The earlier portion of this work was the subject of an unpublished technical memorandum issued in 1973 while the author was at Bell Telephone Laboratories, Murray Hill, NJ. The later portion of this work was supported by the U.S. Department of Energy under Contract No. DE-AC02-76-CHO-3073.

The author is with the Plasma Physics Laboratory, Princeton University, Princeton, NJ 08544.

0018-9480/84/1000-1362$01.00 ©1984 IEEE

overmoded waveguide with a hyperbolic secant curvature variation: one for TE_{10} in rectangular waveguide, and another for HE_{11} in corrugated circular waveguide.

II. The Coupled-Mode Equations

The coupled-mode equations for modes propagating along the waveguide axis (z-direction) are [17], [18]

$$\frac{d}{dz}I_m^+(z) = -\Gamma_m I_m^+(z) + \sum_{n\neq m} K_{mn}^{++} I_n^+(z) + \sum_{n\neq m} K_{mn}^{+-} I_n^-(z)$$

$$\frac{d}{dz}I_m^-(z) = +\Gamma_m I_m^-(z) + \sum_{n\neq m} K_{mn}^{-+} I_n^+(z) + \sum_{n\neq m} K_{mn}^{--} I_n^-(z) \quad (1)$$

where I_m^+ and I_m^- are the complex amplitudes of the forward and reverse traveling modes, respectively. These equations may be derived from Maxwell's equations and are exact, provided that the propagation factors $\Gamma_m = \alpha_m + j\beta_m$ are independent of z [19]. (The Γ_m are functions of z in tapers, for example, where the size of the cross section is changing with z.)

Furthermore, in many cases of interest, the desired mode of propagation (I_0) is far from cutoff. The only significant coupling is to modes that are also far from cutoff, and hence have propagation constants close to that of I_0. For such modes, the coupling coefficients K_{mn}^{+-} and K_{mn}^{-+} are negligible [19], so that reflected power is not important. (The coefficients may not be negligible for coupling to modes close to cutoff, but then their phase constants β_n are much different from β_0 and no significant coupling occurs unless there is a strong discontinuity in the coupling.)

Neglecting reflected modes in (1), therefore, and considering only two modes at a time

$$I_0'(z) = -\Gamma_0 I_0(z) + K_{01} I_1(z)$$
$$I_1'(z) = -\Gamma_1 I_1(z) + K_{10} I_0(z) \quad (2)$$

where the prime denotes differentiation with respect to z, and we have dropped the + superscripts. In order to have power conservation when the attenuation constants α_0 and α_1 are negligible, then, for modes traveling in the same direction, we must have

$$K_{10} = -K_{01}^*. \quad (3)$$

Ordinarily, the coupling factors K_{10} can be factored into the product of a coupling coefficient K derivable from Maxwell's equations and a geometric distortion function $c(z)$ such as curvature, for example. If the distortion were abnormally large, such as in bends with extremely large curvature, then terms that are nonlinear in $c(z)$ would also have to be included in K_{10}. The simple linear term, however, seems to be adequate to account for the data in all practical cases, in which the mode conversion is purposely small.

To simplify the form of (2) to concentrate on mode conversion effects, we factor out the propagation factors of the uncoupled modes in ideal waveguide

$$I_0 = \exp(-\Gamma_0 z) G_0$$
$$I_1 = \exp(-\Gamma_1 z) G_1 \quad (4)$$

and then (2) becomes

$$G_0'(z) = Kc(z) e^{\Delta\Gamma z} G_1(z) \quad (5a)$$
$$G_1'(z) = -K^* c(z) e^{-\Delta\Gamma z} G_0(z) \quad (5b)$$

where

$$\Delta\Gamma = \Delta\alpha + j\Delta\beta = (\alpha_0 - \alpha_1) + j(\beta_0 - \beta_1) \quad (6)$$

and, as discussed in the preceding paragraph

$$K_{01} = Kc(z). \quad (7)$$

In the case of curvature, K is imaginary [19] and z is the arc length along the waveguide centerline.

Now, we take $c(z)$ to have the special form

$$c(z) = R_0^{-1} \operatorname{sech}(kz/2) \quad (8)$$

with $z = 0$ at the center of the coupling region where $c(0) = R_0^{-1}$. A plot of the hyperbolic secant function $\operatorname{sech}(kz/2)$ is presented in Fig. 1. To solve (5) with $c(z)$ as in (8), we first differentiate (5a), substitute (5b) for G_1', and use (5a) itself to write G_1 in terms of G_0 to obtain

$$G_0'' - \left[\frac{c'(z)}{c(z)} + \Delta\Gamma\right] G_0' + |K|^2 c^2(z) G_0 = 0. \quad (9)$$

This equation can be used with the coupling function $c(z)$ in (8), since $c(z)$ in (8) is never exactly zero. Substituting (8) into (9), we obtain

$$G_0'' - \left(\frac{k}{2}\tanh\frac{kz}{2} - \Delta\Gamma\right) G_0' + \left(|K|^2/R_0\right)^2 \operatorname{sech}^2\left(\frac{kz}{2}\right) G_0 = 0. \quad (10)$$

A similar equation may be obtained for G_1 by changing the sign of $\Delta\Gamma$. The solution to (10) is developed in the Appendix.

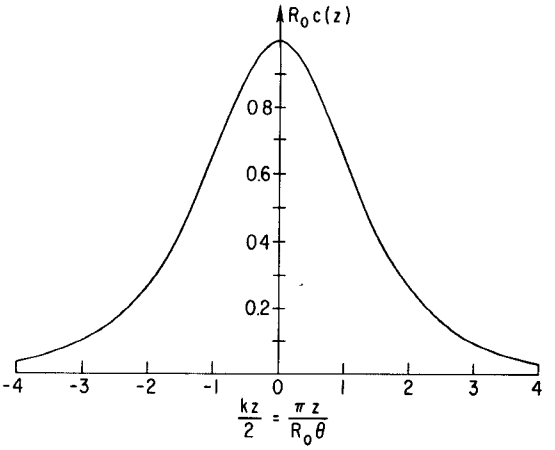

Fig. 1. Hyperbolic secant coupling.

III. Discussion of Solution

A. General

In discussing the solution obtained in the Appendix, it is convenient to introduce the following dimensionless quantities related to the differential attenuation, propagation constant, and the coupling, respectively:

$$A \equiv -\Delta\alpha R_0\theta/2\pi \tag{11a}$$

$$B \equiv \Delta\beta R_0\theta/2\pi \tag{11b}$$

$$C \equiv |K|\theta/\pi. \tag{11c}$$

Here, we have also defined

$$\theta \equiv \int_{-\infty}^{+\infty} c(z)\,dz = 2\pi/(kR_0) \tag{12}$$

making use of (8).

In the case where $c(z)$ represents the curvature in a bend, θ in (32) is simply the total bend angle, and R_0 from (8) is the radius of curvature at the center of the bend $z = 0$. In the general case, define

$$1/R(z) \equiv c(z) = (d\theta/dz) = (1/R_0)\,\mathrm{sech}\left(\pi z/(R_0\theta)\right) \tag{13}$$

using (8) and (12), where

$$1/R_0 = (d\theta/dz)_{z=0}. \tag{14}$$

The case of a twist of total angle θ in rectangular waveguide, for example, can easily be treated with this notation. In that case, $1/R(z)$ is the torsion of the twist.

For convenience, we repeat here the expression for the transmission coefficient T derived in the Appendix (A23). $\Gamma(x)$ is the gamma (factorial) function of the complex argument x [20].

$$T = \frac{\Gamma^2(1/2 + A - jB)}{\Gamma(1/2 + A - jB + C)\Gamma(1/2 + A - jB - C)}. \tag{15}$$

In the case of zero differential attenuation ($\Delta\alpha = 0 = A$), a simple exact expression can be found from (15) for the transmited power $|T|^2$. Write $|T|^2 = T^*T$, note that $\Gamma^*(x^*) = \Gamma(x)$ for an complex x, and use the identity

$$\Gamma\left(\frac{1}{2} + x\right)\Gamma\left(\frac{1}{2} - x\right) = \pi/\cos\pi x. \tag{16}$$

Expanding the resulting products of cosines using ordinary trigonometric identities, we find that the result separates into factors containing B alone and C alone

$$1 - |T|^2 = \sin^2(\pi C)/\cosh^2(\pi B), \qquad \Delta\alpha = 0. \tag{17}$$

Identifying $|T| = |G_0(+\infty)|$ from (A18) and using the fact that

$$|G_0|^2 + |G_1|^2 = 1, \qquad \Delta\alpha = 0 \tag{18}$$

which follows easily from (5), we see that

$$|G_1(+\infty)|^2 = 1 - |T|^2. \tag{19}$$

Hence, (17) represents the power coupled from G_0 to G_1.

The behavior of the transmitted power $|T|^2$ is depicted in Fig. 2 as a function of C for various B. Notice from (17) that $|T|$ is periodic in C, with unity period. In the case of degenerate modes, ($\Delta\beta = 0 = B$), (17) becomes

$$1 - |T|^2 = \sin^2(\pi C), \qquad \Delta\alpha, \Delta\beta = 0. \tag{20}$$

This result can be obtained directly from the coupled-wave equations (5) using definition (11c) for C, and holds for arbitrary coupling $c(z)$. The interesting feature of (17) is that the factor (20) remains intact, and the denominator is independent of C. This result contrasts with the solution in the case of constant coupling [2], where a factor containing B alone cannot be separated out, in general.

In the present case, progressively increasing B from 0 monotonically decreases the amount of power coupled to G_1. Fig. 3 shows that, when B reaches unity or more, very little power is coupled to G_1, and the transmitted power $|T|^2$ is virtually unity, regardless of C.

Mode-selective couplers may be used to couple power from a certain mode in one waveguide through holes or slots to a mode in another waveguide. Ordinarily, these modes have the same propagation constant, so that $\Delta\beta = 0$ and (20) may be used to calculate the coupled power. If one or both coupled waveguides is overmoded, coupling to or from an undesired mode with nonzero $\Delta\beta$ can be calculated from (17), provided the coupling variation follows the hyperbolic secant form defined in (13). This coupling variation can be useful when a broad-band mode-selective coupler must be designed.

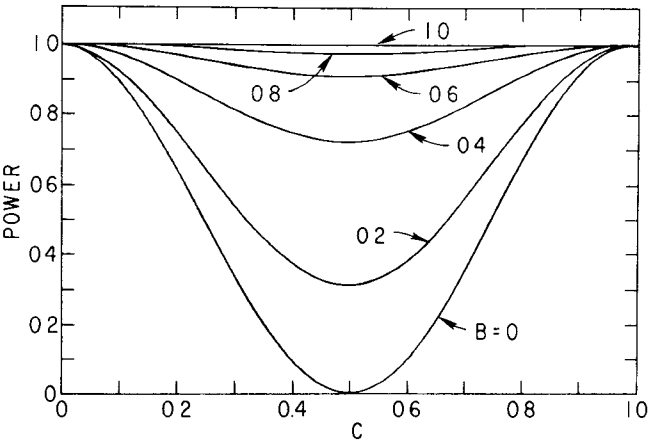

Fig. 2. Transmitted power as a function of the normalized total coupling C when $\Delta\alpha = 0$.

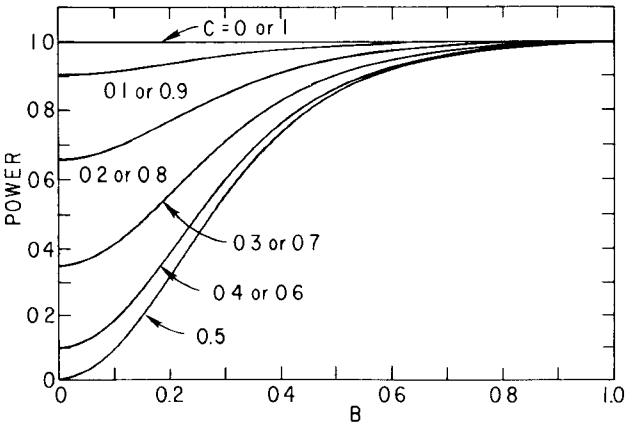

Fig. 3. Transmitted power as a function of the normalized propagation constant when $\Delta\alpha = 0$.

B. Comparison with Perturbation Theory

When $C/B = 2|K|/(\Delta\beta R_0)$ is small and $A = 0$, perturbation theory may be used to find an estimate for $|T|^2$. Small C/B is equivalent to a small amount of coupling in one beat-wavelength $2\pi/\Delta\beta$. The perturbation solution for arbitrary $c(z)$ is [19]

$$1 - |T|^2 \cong \left| \int_{-\infty}^{+\infty} e^{-j\Delta\beta z} |K| c(z)\, dz \right|^2, \qquad \Delta\alpha = 0 \quad (21)$$

which in the present case becomes, using (8) and (11)

$$1 - |T|^2 = (\pi C)^2 / \cosh^2(\pi B), \qquad \Delta\alpha = 0. \quad (22)$$

Notice that this, in general, overestimates the power coupled to G_1, but reduces to the exact result (17) when $C = |K|\theta/\pi$ is small. For comparison, the corresponding coupled power in a bend of constant radius R_0 when $C \ll B$, using (11b) to define B, is [2]

$$1 - |T|^2 = (\pi C)^2 [\sin(\pi B)/(\pi B)]^2. \quad (23)$$

C. Added Heat Loss

No simple trigonometric formula can be derived for $|T|^2$ in the general case when $\Delta\beta = 0$, but $\Delta\alpha \neq 0$. The curves in Fig. 4 were calculated directly from (15) using a computer program for numerical evaluation of the gamma functions [21]. These results were checked against simple formulas which can be derived for the cases $A = 0.5$ and 1.0 using (16). Notice that, for small total coupling C, increasing A from zero increases the transmitted power by breaking the degeneracy $\Delta\Gamma = 0$ between the two modes in a manner similar to Fig. 2. For large C, however, the power never returns competely to G_0 because of the large damping in the coupled mode G_1.

In most practical cases, the differential attenuation is small, and its effect is a small correction to $|T|^2$. In such cases, it is convenient to define an "added heat loss" (A.H.L.) as

$$\text{A.H.L.} \equiv \ln \left| \frac{T(0, B, C)}{T(A, B, C)} \right| \quad (24)$$

where the transmission coefficient T is considered as a function of the three normalized parameters of (11).

When B is large and both A and C are small, an estimate of A.H.L. can be obtained by expanding the gamma functions in (15) using Stirling's approximation. The result is

$$\text{A.H.L.} \cong A(C/B)^2. \quad (25)$$

This result agrees with the following formula for A.H.L. that can be derived from perturbation theory [22], whenever the loss considered as a function of B is maximum near $B = 0$ and is small for all $|B|$ greater than some reasonably small fraction of the actual B

$$\text{A.H.L.} \cong \frac{|\Delta\alpha|}{(\Delta\beta)^2} \int_{-\infty}^{+\infty} |K|^2 c^2(z)\, dz. \quad (26)$$

Equation (25) can be obtained by performing the integration in (26) using (8) and the definition of (11).

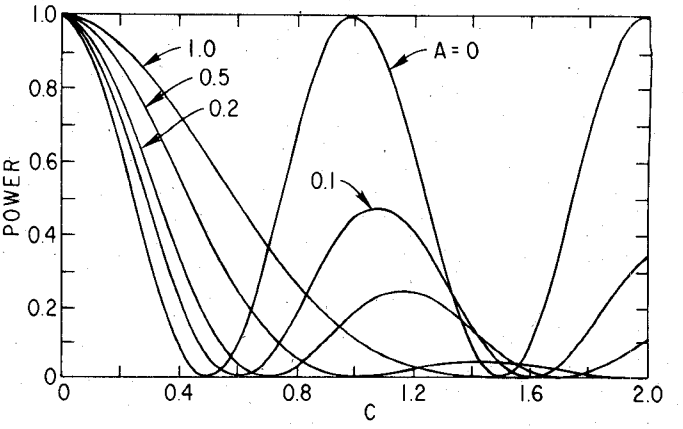

Fig. 4. Transmitted power as a function of C when $B = 0$.

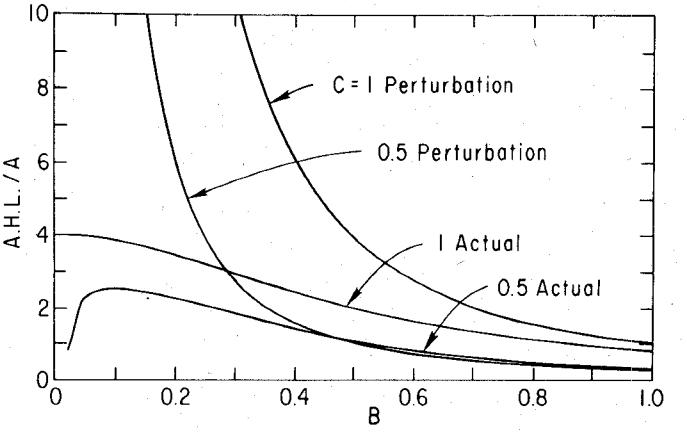

Fig. 5. Ratio of the added heat loss (A.H.L.) to the normalized differential attenuation constant A, as calculated by the exact formula (24) and by perturbation theory (25) for $A = 0.0025$.

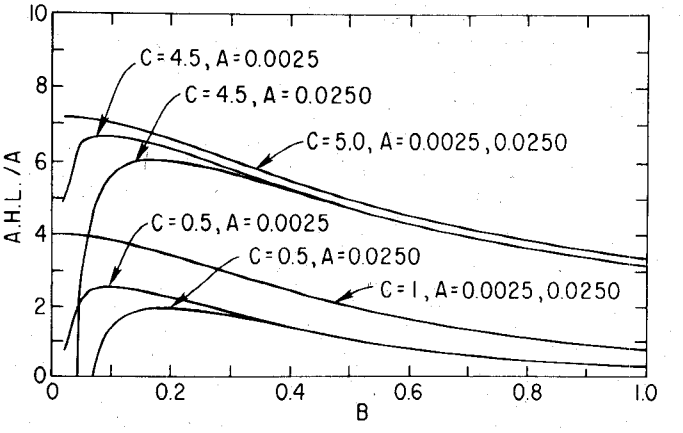

Fig. 6. Ratio of A.H.L. to A as a function of B for various C and A.

A comparison between the approximate expression (25) for A.H.L. and the exact expression (24) evaluated numerically is depicted in Fig. 5 for relatively small coupling C. As in the case of zero $\Delta\alpha$, the perturbation results again overestimate the loss, but reduce to the exact result for small $(C/B)^2$.

Fig. 6 reproduces the exact results of Fig. 5 and compares these with additional results for larger C and A. Notice that the value of A does not affect the added heat loss to A ratio when C is an integer. From (17), it can be

seen that this corresponds to the case of zero transmission loss for arbitrary B when $A=0$. When C takes on half-integral values, on the other hand, the loss from (17) is maximum. In this case, increasing A for very small B tends to decrease the degeneracy between modes and also to decrease the transmission loss (see the discussion of Fig. 4). In such cases, the "added heat loss" can even become negative for larger A, as Fig. 6 shows.

D. Truncation of the Coupling

In practice, it is of course necessary to truncate the hyperbolic secant coupling function $c(z)$ at some finite length. To achieve the same total coupling (which would be the bend angle for curvature coupling, for example), it is necessary to scale the value of θ used in the coupling function (13). If we define L as the total coupling length, and θ_s as the scaled coupling parameter, then we require that

$$\int_{-\infty}^{+\infty} c(z)\,dz = \frac{1}{R_0}\int_{-L/2}^{L/2} \operatorname{sech}(\pi z/R_0\theta_s)\,dz = \theta. \quad (27)$$

Evaluation of the integral in (27) yields an implicit expression for θ_s

$$(2\theta_s/\pi)\arctan\left(\sinh\frac{\pi}{2}\frac{L}{R_0\theta_s}\right) = \theta. \quad (28)$$

When $L/(R_0\theta_s)$ is large, which is usually required for low loss, we may expand the functions in (28) in terms of simple exponentials. Expanding the result about $\theta_s=\theta$, we find

$$\frac{\theta_s}{\theta} \cong \frac{1}{1-1/\left(\frac{\pi}{4}e^x - x\right)} \quad (29)$$

where

$$x \equiv \frac{\pi}{2}\frac{L}{R_0\theta}. \quad (30)$$

Fig. 7 contains a plot of (29) compared with the exact result obtained numerically for the case $\theta=\pi/2$. When $L/R_0 > 2.5$, which is usually required in practice for low loss, the approximate expression is very good.

In Figs. 8 and 9, we provide a basis for choosing the truncated coupling length L. These figures show the situation for $\theta=\pi/2$, and $A=0$, $B=0.5$, and $|C/B|=5$ or 6. For both integral and half-integral C, which correspond to minimum and maximum loss at $L\to\infty$, respectively, L/R_0 must reach about 6 before the loss (coupled power) with truncated coupling approaches the loss for infinite coupling (with no truncation). The actual loss in these figures was calculated numerically from the coupled-mode equations assuming a sharp truncation in the coupling, so that $c(z)$ is given by (8) for $|z| \leqslant L/2$, and $c(z)=0$ for $|z| > L/2$. The straight lines in the figures were calculated from (17).

The actual value of $(L/R_0\theta)$ required for satisfactory results depends on the ratio $|C/B|$. For small values of this ratio, the coupling at the truncation points $z=\pm L/2$ is small and does not strongly affect the overall loss. Hence,

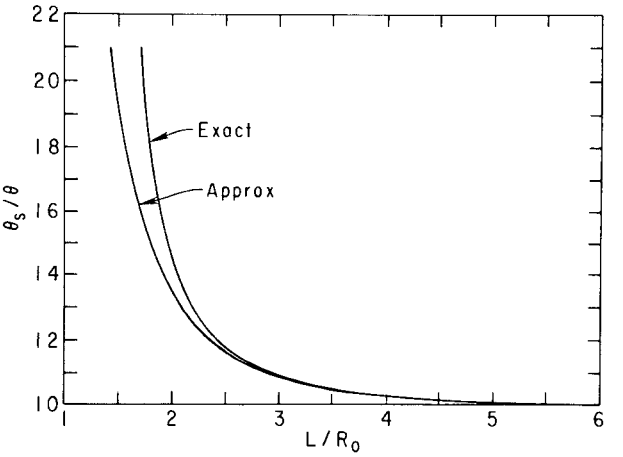

Fig. 7. Approximate (29) and exact ratios of the scaled and desired angles θ_s and θ as a function of the normalized coupling length.

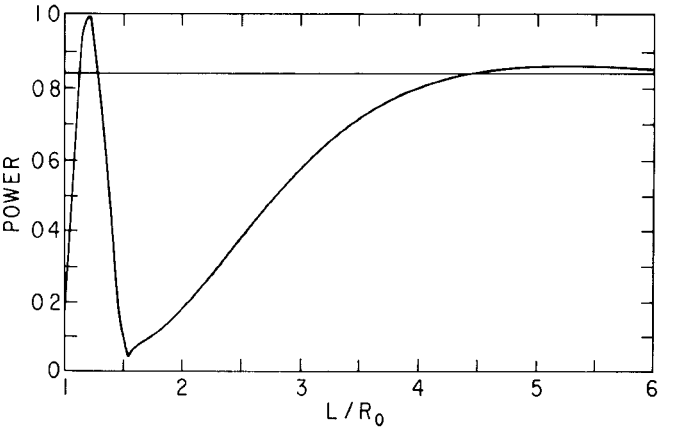

Fig. 8. Transmitted power versus normalized coupling length for $\theta=\pi/2$, $A=0$, $B=0.5$, and $C=2.5$. The straight line is the value for infinite coupling length obtained from (17).

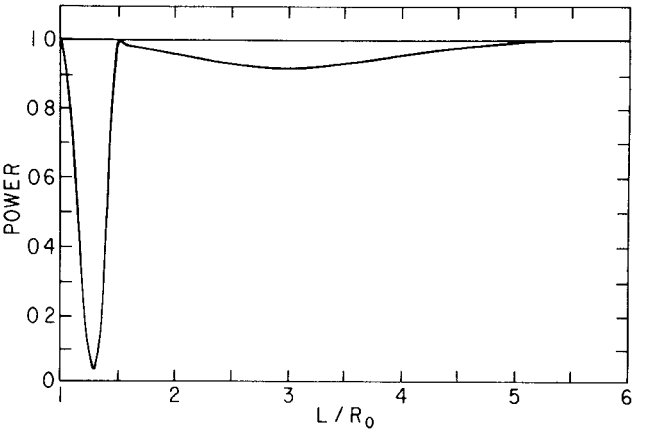

Fig. 9. Transmitted power versus normalized coupling length for $\theta=\pi/2$, $A=0$, $B=0.5$, and $C=3.0$. The straight line is the value obtained from (17).

$L/(R_0\theta)$ can be decreased to make a shorter coupling section. For larger $|C/B|$, the coupling $c(z)$ must be reduced to a small value before truncation, and this implies larger $L/(R_0\theta)$.

If the truncation is not abrupt, on the other hand, the hyperbolic secant coupling length may be reduced slightly.

In general, the strength of the coupling between modes at the truncation region is roughly inversely proportional to the order of the lowest order derivative in the coupling function that is discontinuous. That is, a parabolic taper to zero in $c(z)$ for $|z| > L/2$ is better than a linear taper, which in turn is better than an abrupt truncation. Integration by parts of the integral in the perturbation solution (21) quickly shows this to be true, provided that the length of the taper exceeds a beat-wavelength $2\pi/\Delta\beta$. In physically practical situations involving hyperbolic secant coupling such as in bends or twists, a gradual truncation is actually more natural than an abrupt one.

IV. Application to the Design of Bends

A. Rectangular Waveguide

Overmoded rectangular waveguides are commonly used for the propagation of low-level signals over several meters at millimeter wavelengths, because the losses are lower than in dominant-mode waveguide and because the TE_{10} mode can easily be launched in the larger overmoded waveguide by a taper. To negotiate bends in the H-plane, a quasi-optical miter bend is usually fairly satisfactory, with mode conversion proportional to $(a/\lambda)^{-3/2}$, where a is the length of the wall perpendicular to the E-field [23], [24]. For example, at 140 GHz in WR28 waveguide (0.280 × 0.140 in), the mode conversion in an H-plane 90-degree miter is only 0.3 dB. An E-plane miter, however, would have 1.5 dB of mode conversion loss under these conditions, and the loss varies only as $(b/\lambda)^{-1/2}$, where b is the length of the wall parallel to E [23], [24].

As an alternative to the E-plane miter, a gradual E-plane bend with hyperbolic secant curvature variation was considered. The coupling is from TE_{10} to the TE_{11}/TM_{11} degenerate pair. The total coupling coefficient is given in [25]; when TE_{11}/TM_{11} is well above cutoff, $K \simeq j(4\sqrt{2}/\pi)(b/\lambda)$ [24]. This coupling coefficient is about the same as for TE_{10} to TE_{20} coupling in H-plane bends $K \simeq j(32/9\pi)(a/\lambda)$. Fortunately, however, the total mode conversion in gradual E-plane bends is smaller than in corresponding H-plane bends because the $\Delta\beta$ for the former is larger.

The mode conversion loss in a 6-in E-plane bend in WR28 is shown in Fig. 10. In accordance with the theory, the mode conversion measured at 140 GHz was less than the experimental error, about 0.1 dB. The mode conversion predicted by (17) differs from the result of numerical integration in Fig. 10 at the higher frequencies due to the truncation of the hyperbolic secant curvature at $L/R_0 = x = 4$ [see (29)], and the fact that the coupling factor C in (11c) increases to 3.15 at 300 GHz, while B in (11b) drops to 0.6. Figs. 8 and 9 indicate the discrepancy for similar conditions. In any case, the mode conversion loss for the truncated hyperbolic secant curvature is generally less than that for the a linearly tapered, or triangular, curvature variation suggested in [26]. Not shown in Fig. 10 are the loss for a cosine curvature variation (with zero curvature at both bend ends) [25], almost identical to that of the triangular curvature, and the loss for constant curvature [2], which has nulls at certain frequencies but generally has the highest mode conversion. The ohmic loss for ideal copper conductivity in the 6-in bend increases from 0.09 dB at 100 GHz to 0.13 dB at 300 GHz for the TE_{10} mode. The effect of the differential attenuation $\Delta\alpha$ on the mode conversion is negligible in this case, since a direct computation of (15) showed virtually no difference from (17).

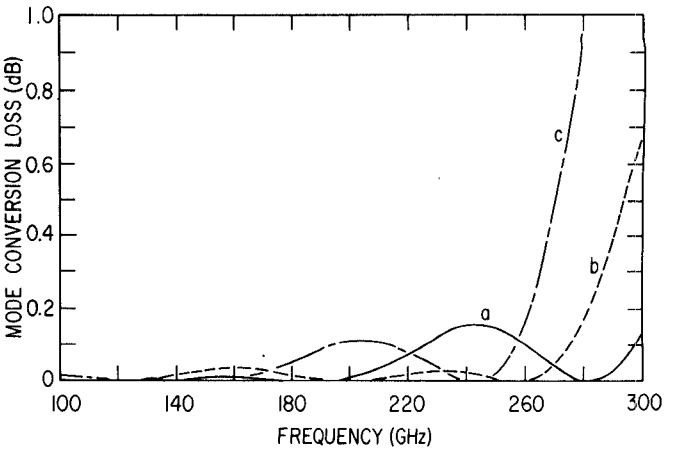

Fig. 10. Losses in 90-degree E-plane bends propagating TE_{10} in WR28 (0.280×0.140 in) rectangular waveguide with 6-in arc length. (a) Loss to TE_{11}/TM_{11} with hyperbolic secant curvature calculated from (15) or (17); (b) Same as (a), but calculated from numerical integration of the coupled wave equations (5) with the curvature truncated at $L/R_0 = 4$; (c) Loss calculated for a triangular curvature variation from numerical integration of (5).

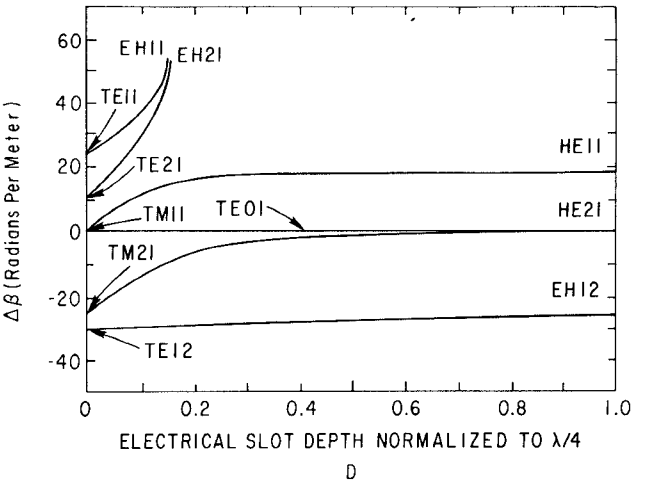

Fig. 11. Propagation constants relative to TE_{01} in 1.094-in I.D. corrugated circular waveguide as a function of effective slot depth at 60 GHz.

B. Corrugated Circular Waveguide

For very low-loss and high-power transmission at millimeter wavelengths, it is necessary to use highly overmoded circular waveguide. Corrugated circular waveguides are particulary convenient, since it supports the polarized HE_{11} mode, which has very low loss [27] and superior radiation properties when launched from the open end of a waveguide [28]. If made flexible, the corrugated waveguide can be formed into compact bends with low mode conversion when propagating HE_{11}. As shown in Fig. 11, the HE_{11} is well separated in β from competing modes, such as TE_{01} and HE_{21}, over a wide range of corrugation depths.

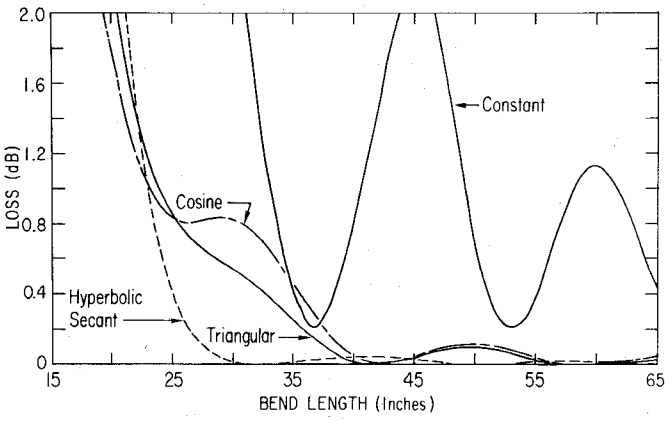

Fig. 12. Losses to TE_{01}, HE_{21}, and HE_{31} in 90-degree H-plane bends propagating HE_{11} in 1.094-in circular waveguide with an electrical corrugation (slot) depth of 0.5 ($\lambda/4$) at 60 GHz; $L/R_0 = 4$ for the hyperbolic secant curve.

The superiority of the hyperbolic secant curvature variation for a 90-degree H-plane bend propagating HE_{11} in 1.094-in-diameter waveguide is evident from Fig. 12. The reason, evidently, is that the coupling parameter C in (11c) for this diameter and frequency is almost exactly 2 for coupling from HE_{11} to either TE_{01} or HE_{21} [29]. The mode conversion loss predicted by (17) is then virtually zero, independent of bend length.

The deviations from zero in the curve in Fig. 12 calculated from numerical integration of the coupled-mode equations are caused by the truncation of the hyperbolic secant variation ($L/R_0 = 4$ is assumed for all L in Fig. 12) and by the need to consider simultaneous coupling to both TE_{01} and HE_{21}. For bend lengths less than 25 in, coupling through HE_{21} to HE_{31} also becomes important. Nevertheless, the losses in Fig. 12 are much less than those predicted by the approximate (perturbation) formula (22). For $L = 32$ in, for example, the coupling parameter B is approximately 1, $C = 2$, and the loss to either TE_{01} or HE_{21} calculated from (22) would be 2 dB.

A corrugated waveguide bend with a hyperbolic secant curvature variation corresponding to the parameters in Fig. 12 was fabricated with $L = 32$ in for use in electron–cyclotron heating on Princeton's PLT and PDX tokamaks [30] (Fig. 13). In this application, up to 200 kW must be propagated around tight corners near the tokamaks. The H-plane mode conversion for this bend measured at low power was less than 0.1 dB when propagating HE_{11}, between 59 and 60 GHz. (HE_{11} launchers for this experiment are described in [31].) Measured mode conversion when the same bend was used in an E-plane configuration was also less than 0.1 dB. In that case, coupling to TM_{02} replaces coupling to TE_{01} [32]. The experimental results apparently confirm the superiority of the hyperbolic secant curvature variation for this application as indicated theoretically by Fig. 12.

Because HE_{11} is separated so far from other modes in $\Delta\beta$ over such a wide range of corrugation depths (see Fig. 11; β for TM_{02} is less than that for TE_{01} for all corrugation depths up to a quarter wavelength), it might be expected that both E and H plane bends would have low loss over a fairly large bandwidth, and this is demonstrated theoretically in Fig. 14 from numerical integration of the coupled-mode equations (5) for an H-plane bend. (The theoretical E-plane loss is slightly less up to 70 GHz and then slightly higher.) Only at the high frequencies do the $\Delta\beta$ become too small for the denominator in (17) to overcome the variations in the numerator.

The situation for propagation of TE_{01} in corrugated bends in entirely different. In that case, it is generally disastrous to have corrugations near a quarter wavelength deep, because energy is efficiently coupled through HE_{11}

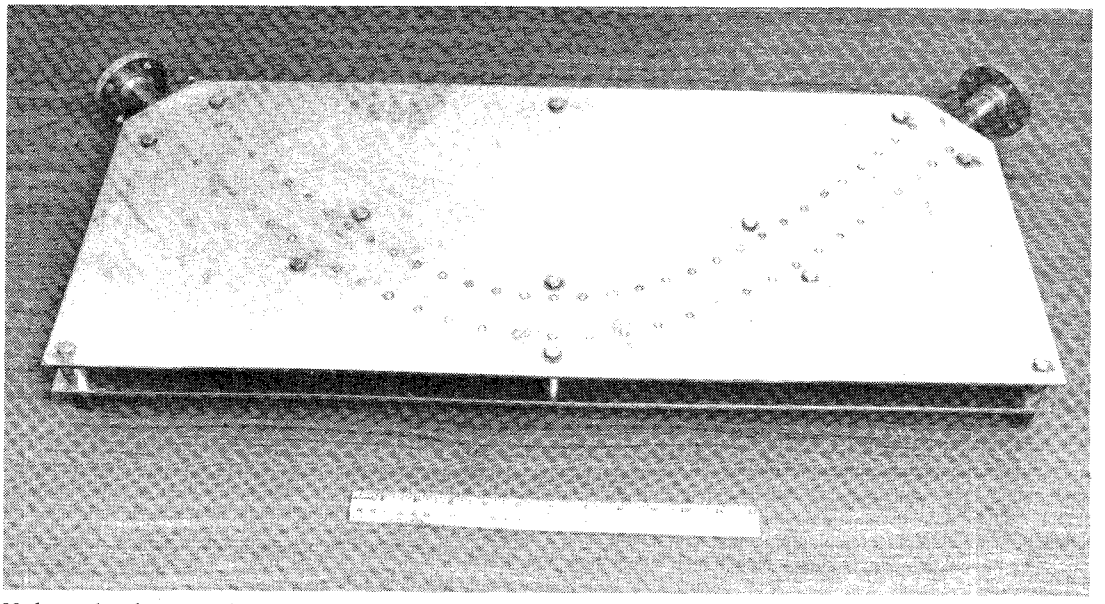

Fig. 13. A 90-degree bend propagating HE_{11} in 1.094-in-diameter corrugated waveguide with hyperbolic secant curvature variation over a 32-in arc length. $R_0 = 8$ in.

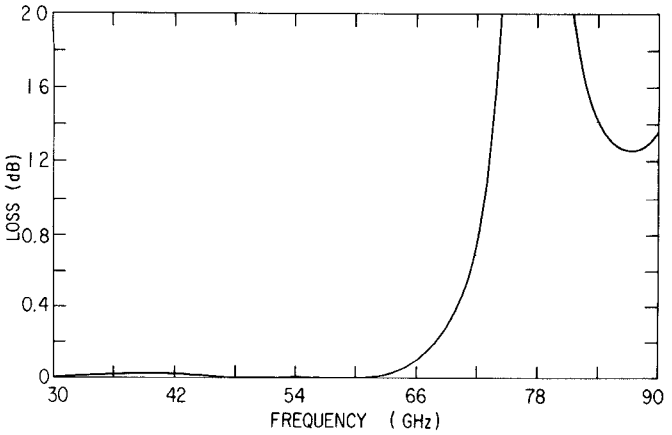

Fig. 14. Loss to TE_{01}, HE_{21}, and HE_{31} in a 90-degree hyperbolic secant H-plane bend propagating HE_{11} in 1.094-in corrugated waveguide with a mechanical corrugation depth of $\lambda/4$ at 73 GHz and a corrugation period twice the corrugation width; $L/R_0 = 4$.

into HE_{21}, which becomes nearly degenerate with TE_{01} [33] ($\Delta\beta \simeq 0$; See Fig. 11). The corrugations must also not be too shallow, since HE_{11} itself then approaches degeneracy with TE_{01}, becoming TM_{11} in smooth waveguide with $\Delta\beta = 0$ (Fig. 11). A fairly narrow region of slot depth over which there is low mode conversion then appears and the bend lengths for which the mode conversion is acceptably low become much longer than for bends propagating HE_{11}.

Numerical integration of the coupled mode equations for TE_{01} bends at 60 GHz in 1.094-in-diameter waveguide showed that the cosine curvature variation is superior at most corrugation depths to a hyperbolic secant variation and also to the triangular variation, which behaves almost identically to a cosine squared variation. Experimental measurements on several bends confirmed this picture [30].

Appendix

To solve (1), we transform it to a differential equation whose solutions are hypergeometric functions [34].[1] The required transformation is easier to follow if we start from the hypergeometric differential equation and work back to (10). The general second-order hypergeometric equation may be written as follows [35]:

$$(\Omega - \rho_1)(\Omega - \rho_2)F(\xi) = \xi(\Omega + \sigma_1)(\Omega + \sigma_2)F(\xi) \tag{A1}$$

where Ω is the operator

$$\Omega \equiv \xi \frac{d}{d\xi} \tag{A2}$$

and ρ_1, ρ_2, σ_1, and σ_2 are complex constants.

If we make the substitutions

$$\xi = -\exp(+kz) \tag{A3}$$

and

$$F[\xi(z)] = f(z)G_0(z) \tag{A4}$$

then (A1) becomes

$$G_0''\left[2\frac{f'}{f} + k\frac{(r_1 - \xi s_1)}{(1-\xi)}\right]G_0' + \left[\frac{f''}{f} + k\frac{f'}{f}\frac{(r_1 - \xi s_1)}{(1-\xi)} + \frac{k^2(r_1 - \xi s_2)}{(1-\xi)}\right]G_0 \tag{A5}$$

where the prime denotes differentiation with respect to z and

$$r_1 = -\rho_1 - \rho_2, \; r_2 = \rho_1\rho_2 \tag{A6}$$

$$s_1 = \sigma_1 + \sigma_2, \; s_2 = \sigma_1\sigma_2. \tag{A7}$$

At this point, we choose $f(z)$ to have the special form

$$f[z(\xi)] = (-\xi)^{-r_0/2}(1-\xi)^{(r_0 - s_0)/2}. \tag{A8}$$

Recognizing from (A3) that

$$\xi/(1-\xi) = -\frac{1}{2}\left(1 + \tanh\frac{kz}{2}\right) \tag{A9}$$

and

$$\xi/(1-\xi)^2 = -\frac{1}{4}\operatorname{sech}^2\frac{kz}{2} \tag{A10}$$

we then find that the first derivative terms in (A5) and (10) can be made equal, provided that

$$r_0 - r_1 = \frac{1}{2} + (\Delta\Gamma/k) \tag{A11a}$$

$$s_1 - s_0 = \frac{1}{2} - (\Delta\Gamma/k). \tag{A11b}$$

With the help of a partial fraction expansion involving terms in $(1-\xi)^{-m}$, $m = 0,1,2$, and again making use of (A9) and (A10), we find that the terms multiplying G_0 in (A5) and (10) can be made equal provided that

$$\frac{1}{4}r_0^2 - \frac{1}{2}r_0r_1 + r_2 = 0 \tag{A11c}$$

$$\frac{1}{4}(r_0^2 - s_0^2) + \frac{1}{2}(s_0s_1 - r_0r_1) + (r_2 - s_2) = 0 \tag{A11d}$$

and

$$\frac{1}{4}(s_0 - r_1)[(s_0 - r_0) + 2(1 + r_1 - s_1)] = -4|K|^2/(kR_0)^2. \tag{A11e}$$

Through (A11), (A6), and (A7), we can now relate the parameters in (A1) to those of our original differential (10), thus essentially completing the transformation. Before we can solve explicitly for ρ_1, ρ_2, σ_1, and σ_2, however, we need some more information, which we can obtain by examining the form of the solutions to (A1).

The solutions to (A1) have the form of normal modes in the limit of large $|z|$. Near $\xi = 0$ ($z = -\infty$), one solution to (A1) has the form

$$F_1^-(z) = (-\xi)^{+\rho_1}_{(2)}F_1(\rho_1 + \sigma_1, \rho_1 + \sigma_2; \rho_1 - \rho_2 + 1; \xi) \tag{A12}$$

while another independent solution $F_2^-(\xi)$ can be obtained by interchanging ρ_1 and ρ_2 in (A12). The hypergeometric functions ${}_2F_1$ are expressable as power series that reduce

[1] An equation with certain similarities to (10) and describing the propagation and reflection of obliquely incident electromagnetic waves in a plane-stratified isotropic plasma has also been solved by this type of transformation.

to the value unity in the limit of small argument. From (A3), we then see that the leading term in (A12) is $\exp(-k\rho_1 z)$, which represents a normal mode if ρ_1 is imaginary.

Similarly, we may write the solutions for $|\xi|>1$

$$F_1^+(\xi)=(-\xi)^{-\sigma_1}F_1(\sigma_1+\rho_1,\sigma_1+\rho_2;\ \sigma_1-\sigma_2+1;\xi^{-1}). \quad \text{(A13)}$$

An interchange of σ_1 with σ_2 yields $F_2^+(\xi)$. Because of the ξ^{-1} argument, these functions now reduce to unity when ξ approaches minus infinity ($z\to+\infty$). Again, from (A3) it is evident that the leading term in (A13) has normal mode form when σ_1 is imaginary.

In view of (A4), (A8), and (A3), we thus find the following possible limiting forms for G_0, where we define $G_{0i}^{\pm}=F_i^{\pm}(\xi)/f(\xi)$, $i=1,2$:

$$\lim_{z\to-\infty}G_{01}^-(z)=\lim_{\xi\to 0}F_1^-(\xi)/f(\xi)=\exp\left[k\left(\frac{r_0}{2}+\rho_1\right)z\right] \quad \text{(A14a)}$$

$$\lim_{z\to+\infty}G_{01}^+(z)=\lim_{\xi\to-\infty}F_1^+(\xi)/f(\xi)=\exp\left[k\left(\frac{s_0}{2}-\sigma_1\right)z\right] \quad \text{(A14b)}$$

$$\lim_{z\to+\infty}G_{02}^+(z)=\lim_{\xi\to-\infty}F_2^+(\xi)/f(\xi)=\exp\left[k\left(\frac{s_0}{2}-\sigma_2\right)z\right]. \quad \text{(A14c)}$$

Since the coupling function $c(z)$ from (8) approaches zero for large $|z|$, we must pick the solutions so that G_0' vanishes [see (5a)]. Therefore, the exponents in (A14a) and (A14b) must also vanish

$$\frac{r_0}{2}+\rho_1=0 \quad \text{(A15)}$$

$$\frac{s_0}{2}-\sigma_1=0. \quad \text{(A16)}$$

In the usual mode conversion problems, one mode starts with all the power. We take G_0 to be this mode, and $G_{01}^-(z)$ with unit amplitude then represents the solution at $z=-\infty$. There are no other waves present in this limit, since the coupled mode equations (5) do not allow for reflections. The amplitude of $G_{01}^+(z)$ at $z=+\infty$ then represents the transmission coefficient for G_0. Because $G_{02}^+(z)$ has a nonvanishing exponent at $z=+\infty$, it cannot be part of the solution for G_0 in that limit. In fact, we will see that the exponent is negative and hence G_{02}^+ goes to zero as z goes to infinity.

To find the transmission coefficient T, we need to find an analytic solution of (A1), valid for all ξ, that will reduce to F_1^- for $|\xi|<1$ and to a linear combination of F_1^+ and F_2^+ for $|\xi|>1$. Such a solution can be found in terms of Meijer's G-functions, which are expressible as Barnes contour integrals [36]. The desired solution to (A1) is

$$F(\xi)=\frac{\Gamma(1-\rho_1-\rho_2)}{\Gamma(\rho_1+\sigma_1)\Gamma(\rho_1+\sigma_2)}\frac{1}{2\pi j}\cdot\int_{L_c}\frac{\Gamma(\rho_1-w)\Gamma(\sigma_1+w)\Gamma(\sigma_2+w)}{\Gamma(1-\rho_2+w)}(-\xi)^w\,dw \quad \text{(A17)}$$

where the contour L_c goes from $w=-j\infty$ to $w=+j\infty$ in a manner such that all the poles of $\Gamma(\rho_1-w)$ lie to the right of the contour, and all the poles of $\Gamma(\sigma_i+w)$, $i=1,2$ lie to the left of the contour. $\Gamma(x)$ is the gamma function of the complex argument x [20]. It is assumed that $1-\sigma_m-\rho_n$ is not a positive integer for $m,n=1,2$. The integral in (A17) converges if $|\arg\xi^{-1}|<\pi$. Notice from (A3) that (A17) resembles a bilateral inverse Laplace transform for F considered as a function of z.

To evaluate (A17) for $|\xi|<1$, we may close the contour L_c in the right-half w-plane without affecting the value of the solution. The evaluation of this closed contour integral in terms of the residues of gamma functions yields the infinite power series denoted by (A12). Similarly, we may close the contour in the left-hand w-plane when $|\xi|>1$. The coefficient of the power series denoted by (A13) is then the transmission coefficient T, which we find to be

$$T=\frac{\Gamma(1-\rho_2+\rho_1)\Gamma(\sigma_2-\sigma_1)}{\Gamma(1-\rho_2-\sigma_1)\Gamma(\sigma_2+\rho_1)}=G_0(+\infty). \quad \text{(A18)}$$

To find T explicitly in terms of the parameters of the coupling function (8), we need now only solve (A11) with (A15) and (A16) to obtain the quantities appearing in (A18). It turns out that the ρ_i and σ_i cannot all be specified uniquely since we have an insufficient number of constraints, but T nevertheless is uniquely determined. Using (A15) and (A16), and the definitions (A6) and (A7), we find from (A11a) and (A11b)

$$\sigma_2-\sigma_1=\frac{1}{2}-\frac{\Delta\Gamma}{k}=1-\rho_2+\rho_1. \quad \text{(A19)}$$

Similarly, from (A11e) we obtain another relation, which when combined with (A19), yields

$$(\sigma_1+\rho_1)=\pm 2|K|/(kR_0) \quad \text{(A20)}$$

and

$$(1-\rho_2-\sigma_2)=\mp 2|K|/(kR_0). \quad \text{(A21)}$$

Alternately adding and subtracting (A20) and (A21) and combining the results, we find

$$1-\rho_2-\sigma_1=\frac{1}{2}-\Delta\Gamma\mp 2|K|/(kR_0) \quad \text{(A22a)}$$

and

$$\sigma_2+\rho_1=\frac{1}{2}-\Delta\Gamma\pm 2|K|/(kR_0). \quad \text{(A22b)}$$

The final result for T is, from (A18), (A19), and (A22), regardless of whether the upper or lower signs are chosen in (A22)

$$T=\frac{\Gamma^2(1/2+A-jB)}{\Gamma(1/2+A-jB+C)\Gamma(1/2+A-jB-C)}. \quad \text{(A23)}$$

Here, we have defined the normalized quantities A, B, and C as in (11).

In order that the residual solution G_{02}^+ vanish as z approaches $+\infty$, as discussed earlier, the real part of the exponent in (A14c) must be negative. From (A16), (A19),

(12), and (6), this requires that

$$0 < \mathrm{Re}\left(\frac{1}{2} + A - jB\right) = \frac{1}{2} + A. \qquad \text{(A24)}$$

Notice that this condition also ensures that T in (A23) has no poles. In the usual cases of interest, $\Delta\alpha$ is negative because the desired mode G_0 has lower loss than the spurious mode G_1. Then, (A24) is automatically satisfied.

References

[1] H. E. Rowe, "Approximate solutions for the coupled line equations," *Bell System Tech. J.*, vol. 41, pp. 1011–1029, May 1962.

[2] S. E. Miller, "Coupled wave theory and waveguide applications," *Bell System Tech. J.*, vol. 33, pp. 661–720, May 1954.

[3] R. B. Smith, "Analytical solutions for linearly tapered directional couplers," *J. Opt. Soc. Am.*, vol. 66, pp. 882–892, Sept. 1976.

[4] R. A. Waldron, "The theory of coupled modes," *Quart. J. Mech. Appl. Math.*, vol. 18, pp. 385–404, 1965.

[5] S. E. Miller, "On solutions for two waves with periodic coupling," *Bell System Tech. J.*, vol. 47, pp. 1801–1822, Oct. 1968.

[6] A. L. Cullen and O. J. Davies, "Periodic coupling of waveguide modes," *Proc. Inst. Elec. Eng.*, vol. 117, pp. 2061–2069, Nov. 1970.

[7] H. E. Rowe and D. T. Young, "Transmission distortion in multimode random waveguides," *IEEE Trans. Microwave Theory Tech.*, vol. MTT-20, pp. 349–365, June 1972.

[8] L. Solymar, "Design of a conical taper in circular waveguide system supporting H_{01} mode," *Proc. IRE*, vol. 46, pp. 618–619, Mar. 1958.

[9] L. Solymar, "Mode conversion in pyramidal-tapered waveguides," *Electronic and Radio Engineer*, vol. 36, pp. 461–463, Dec. 1959.

[10] H.-G. Unger, "Circular waveguide taper of improved design," *Bell System Tech. J.*, vol. 37, pp. 899–912, July 1958.

[11] F. Sporleder and H.-G. Unger, *Waveguide Tapers Transitions and Couplers*. London: Institution of Elec. Eng., 1979.

[12] W. K. Burns, A. F. Milton, and A. B. Lee, "Optical waveguide parabolic coupling horns," *Appl. Phys. Lett.*, vol. 30, pp. 28–30, Jan. 1977.

[13] J. L. Doane, "Parabolic tapers for overmoded waveguides," *Int. J. Infrared Millimeter Waves*, vol. 5, pp. 737–751, May 1984.

[14] R. P. Hecken, "A near-optimum matching section without discontinuities," *IEEE Trans. Microwave Theory Tech.*, vol. MTT-20, pp. 734–739, Nov. 1972.

[15] R. A. Waldron, "The Theory of Reflections in a Tapered Waveguide," *Radio Electron. Eng.*, vol. 32, pp. 245–254, Oct. 1966.

[16] M. D. Abouzahra and L. Lewin, "Coupling of degenerate modes on curved dielectric slab sections and application to directional couplers," *IEEE Trans. Microwave Theory Tech.*, vol. MTT-28, pp. 1096–1101, Oct. 1980.

[17] S. A. Schelkunoff, "Conversion of Maxwell's equations into generalized telegraphist's equations," *Bell System Tech. J.*, vol. 34, pp. 995–1043, Sept. 1955.

[18] S. P. Morgan, "Theory of curved circular waveguide containing an inhomogeneous dielectric," *Bell System Tech. J.*, vol. 36, pp. 1209–1251, Sept. 1957.

[19] H. E. Rowe and W. D. Warters, "Transmission in multimode waveguide with random imperfections," *Bell System Tech. J.*, vol. 41, pp. 1031–1170, May 1962.

[20] M. Abramowitz and I. A. Stegun, Eds., *Handbook of Mathematical Functions*. Washington, D.C.: U.S. Government Printing Office, 1964.

[21] C. Lanczos, "A precision approximation of the gamma function," *SIAM J. Numer. Anal.*, vol. 1, pp. 86–96, 1964.

[22] D. T. Young, "Effect of differential loss on approximate solutions to the coupled line equations," *Bell System Tech. J.*, vol. 42, pp. 2787–2793, Nov. 1963.

[23] B. Z. Katsenelenbaum, "Diffraction on plane mirror in broad-waveguide junction," *Radio. Eng. Electron. Phys. (USA)*, vol. 8, pp. 1098–1105, July 1963.

[24] J. P. Quine, "Oversize tubular metallic waveguides," in *Microwave Power Engineering*, vol. 1, E. C. Okress, Ed. New York: Academic Press, 1968, pp. 178–213.

[25] J. P. Quine, "*E*- and *H*-plane bends for high-power oversized rectangular waveguide," *IEEE Trans. Microwave Theory Tech.*, vol. MTT-13, pp. 54–63, Jan. 1965.

[26] H.-G. Unger, "Normal mode bends for circular electric waves," *Bell System Tech. J.*, vol. 36, pp. 1292–1307, Sept. 1957.

[27] P. J. B. Clarricoats, A. D. Olver, and S. L. Chong, "Attenuation in corrugated circular waveguides, Part 1. Theory," *Proc. Inst. Elec. Eng.*, vol. 122, pp. 1173–1183, Nov. 1975.

[28] B. MacA. Thomas, "Theoretical performance of prime focus paraboloids using cylindrical hybrid-mode feeds," *Proc. Inst. Elec. Eng.*, vol. 118, pp. 1539–1549, Nov. 1971.

[29] J. L. Doane, "Propagation and mode coupling in corrugated and smooth wall circular waveguides," in *Infrared and Millimeter Waveguides*, vol. 13, K. J. Button, Ed. New York: Academic Press, to be published.

[30] J. L. Doane, "Overmoded waveguide components for the ECH system on PDX," in *Proc. Tenth Symp. on Fusion Eng.*, 1983, pp. 1459–1464.

[31] J. L. Doane, "Mode converters for generating the HE_{11} (gaussian-like) mode from TE_{01} in a circular waveguide," *Int. J. Electron.*, vol. 53, pp. 573–585, Dec. 1982.

[32] P. J. B. Clarricoats, A. D. Olver, and S. L. Chong, "Attenuation in corrugated circular waveguides, Part 2. Experiment," *Proc. Inst. Elec. Eng.*, vol. 122, pp. 1180–1186, Nov. 1975.

[33] J. W. Carlin and S. C. Moorthy, "TE_{01} transmission in waveguide with axial curvature," *Bell System Tech. J.*, vol. 56, pp. 1849–1872, Dec. 1977.

[34] J. Heading, "Polarization of obliquely reflected waves from an isotropic plane-stratified plasma," *Radio Sci.*, vol, 4, pp. 441–447, May 1969.

[35] E. T. Copson, *Theory of Functions of a Complex Variable*. Oxford: University Press, 1935.

[36] Y. L. Luke, *The Special Functions and Their Approximations*, Vol. I. New York: Academic Press, 1969.

John L. Doane (S'66–M'66) was born in New York City, NY, on June 20, 1942. He received a B.E. from Yale University, New Haven, CT, in 1964 and the Ph.D. degree from M.I.T., Cambridge, MA, in 1970.

From 1970 to 1977, he worked at Bell Laboratories, where he made measurements and analyses of mode conversion for long-distance millimeter waveguide communication systems, and worked on the design of an automated microwave transmission surveillance system. Since 1977, he has been designing millimeter-wave instrumentation and low-loss waveguide components for plasma diagnostics and heating at the Plasma Physics Laboratory of Princeton University, Princeton, NJ.